ADVANCED ENGINEERING MATERIALS

DOI: 10.1002/adem.201600646

Lattice Materials with Reversible Foldability**

By *Hamid Ebrahimi, Davood Mousanezhad, Babak Haghpanah, Ranajay Ghosh* and *Ashkan Vaziri**

The authors introduce a new class of lattice materials, where a controlled simultaneous folding of the lattice walls results in a significant size reduction while preserving the overall shape of the original lattice. This reversible folding scheme results in 67 and 50% reduction in size at each level for lattices with triangular and square grid topologies, respectively, while the design enables multiple levels of folding to achieve a desired final size. The authors study the elastic properties and the phononic band structure of the lattice at different stages of folding, using analytical and finite element methods. The proposed concept provides new opportunities for the development of multifunctional deployable structures through significant changes in the size and properties of lattice materials by folding.

The properties of traditional materials are primarily determined by their atomic or molecular arrangements, which are typically difficult to modify due to constraints on sub-continuum forces in the material lattice and relatively closely packed microstructure. Lattice materials, whose structure is obtained through a tessellation of a fundamental geometrical unit cell can be seen as analogs of natural crystals at macroscale and, thus, serve as an excellent template for metamaterial development.[1] More importantly, the meso-level organization and abundant free space inside cellular structures make imparting real-time geometrical changes in their underlying structure (thus their overall properties) much easier compared to traditional monolithic materials or composites. Moreover, if the change in their size and shape are brought about through a controllable mean, a systematic control of their property can be affected, thereby, fostering concerted programmability of a variety of properties and responses.[2] Reflecting the importance of structural programmability, there has been a surging interest in recent times in incorporating this concept across a number of scientific disciplines including robotics,[3] foldable substrates,[4–6] deployable structures,[7,8] advanced manufacturing,[9] lab-on-a-chip systems,[10] and medical devices.[11]

In an early work, You And Pellegrino[12,13] proposed a general concept for deployable structures based on a three dimensional pantograph, that is, deployed and stiffened by means of cables and applied it to the design of deployable mast[12] and support structure for a large mesh reflector.[13,14] There are also other technologies to deploy large booms and masts for astrophysics missions' applications,[8] such as Telescopic and inflatable booms,[15] shape memory composite booms,[16] and deployable truss structures,[17] as well as deployable structures based on using scissor-like elements.[18] More recently, designing foldable structures using origami principles has attracted considerable attention.[19] Silverberg et al.[4] developed a reprogrammable mechanical metamaterial that can be folded based on origami design principles, and so its compressive modulus can be tuned reversibly. Same concept has been used to propose programmable self-folding structures[6,20] with applications in self-folding machines.[5]

The inherently low volume fraction and ordered tessellated organization of lattice materials can be exploited to obtain significant topological (and thus behavior) changes by folding and unfolding of the individual segments of the lattice. In the current paper, we introduce a novel self-replicating and reversible folding scheme for lattice materials. This folding scheme relies on the rotation of the segments that can be achieved either unassisted or assisted with active actuating units. This scheme can be envisioned on a 2×2 tessellation of

[*] *Prof. A. Vaziri, Dr. H. Ebrahimi, Dr. D. Mousanezhad*
Department of Mechanical and Industrial Engineering, Northeastern University, 360 Huntington Ave, Boston, MA
E-mail: vaziri@coe.neu.edu
Dr. B. Haghpanah
Department of Mechanical and Aerospace Engineering, University of California, Irvine, CA 92697, USA
Prof. R. Ghosh
Department of Mechanical and Aerospace Engineering, University of Central Florida, Orlando, FL 32816, USA

[**] *This report was made possible by a NPRP award [NPRP 7-882-2-326] from the Qatar National Research Fund (a member of the Qatar Foundation). The statements herein are solely the responsibility of the authors. (Supporting Information is available online from the Wiley Online Library or from the author).*

square unit cells as shown in Figure 1a. The walls of the unit cells are comprised of multiple one-dimensional sub-segments connected through pin joints, which would allow for their free relative rotation (See Supporting Information). The folding scheme commences with opposite rotations of adjacent vertices of each sub-grid square, as shown by the colored arrows in Figure 1a-1. In the present study, rotations have been applied manually, however, in principal it could be done using servo motors or other actuators. As these rotations progress, the entire lattice begins to morph to maintain compatibility at the joints (Figure 1a-2). It is clear from this figure that two of the opposing mid-points (pin-joints) of each square begin to draw closer to each other, whereas the other pair begin to separate from each other. Note that each point of the mutually closing pair in each square simultaneously serves as a point of mutually separating pair in an adjacent cell, while the opposite is true for the mutually separating pair. This transition continues until the mutually closing pair of points meet, thereby, dividing each square in the original lattice to two smaller squares at each folding level, as seen in Figure 1a-3 (See video in Supporting Information). Note, the distinct rotation of the axes of symmetry of the structure and the unit cells by 45° at the end of the transition. This process can be repeated (Figure 1a-4 and 1a-5) to yield further reduction in the lattice area. There are certain distinctions between the folding schemes of the square and triangular grids, shown in Figure 1b. Compared to the case of a square grid with one active hinge on each cell wall at each folding level, every side of the triangular grid breaks into three equal sized segments, requiring two active pin-joints on each cell wall for each folding level. Furthermore, during the closure phase of each folding level of a triangular grid a set of three points, one hinge from each side of the triangles, touch each other, resulting in more reduction in the size of the lattice compared to a square lattice. Also, note the 30° rotation of symmetry axes of the triangular lattice after each level of folding.

The described folding transitions result in 50 and 67% reduction in the effective area of the square and triangular lattices, respectively. This simple control on the final size and shape of the lattice can be exploited to herald more complex shapes and sizes, while still using relatively primitive base lattice geometry. In Figure 2, we show an example of the potential of this geometric transformation in expanding complex large geometries (letters NU in the figure) from a small base lattice. This figure shows schematics and the corresponding experimental images of two different structures with square and triangle based lattices during two orders of unfolding. This approach can be theoretically utilized to find appropriate deploying plans for any given two dimensional shape, as demonstrated for a tessellated lattice representing the United States map in Figure 3. Although, area reduction in the folding process does not depend on the direction of rotation of the nodes (i.e., clockwise or counter clockwise), it can affect the shape of the final folded structure. For structures with relatively small number of mesh, the sequence of rotation directions will determine the shape of the folded lattice, however, for large lattices the overall shape will be nearly preserved during folding for all combination of rotations (see the Supporting Information). In other words, for an infinite lattice, the final shape does not depend on the sequence of rotation directions, whereas for the case of a finite lattice, the shape of the boundary of the final configuration is indeed a function of the sequence of rotation directions. In the supporting information, we present a numerical algorithm for the design of reversible foldable lattice structures based on square or equilateral triangular elements to achieve any target geometry through folding. This high degree of geometrical change can yield a correspondingly wide bracket of behavior. In the following sections, we investigate the quasi-static elastic and phononic behavior of square grid lattices during different stages of folding and unfolding transition. While in the rest of the paper, we focus on square grid lattices, similar conclusions and discussions are applicable to lattice materials

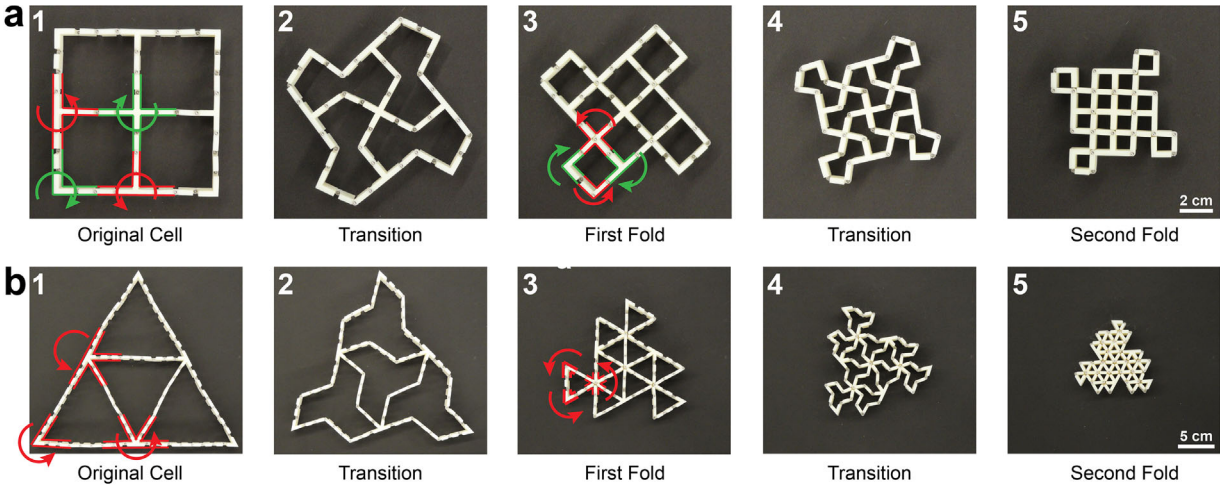

Fig. 1. 3D printed specimens demonstrating the proposed folding scheme in square (a) and triangular (b) lattices, which are folded twice, allowing 50 and 67% reductions in the effective area of the lattice at each level of folding, respectively.

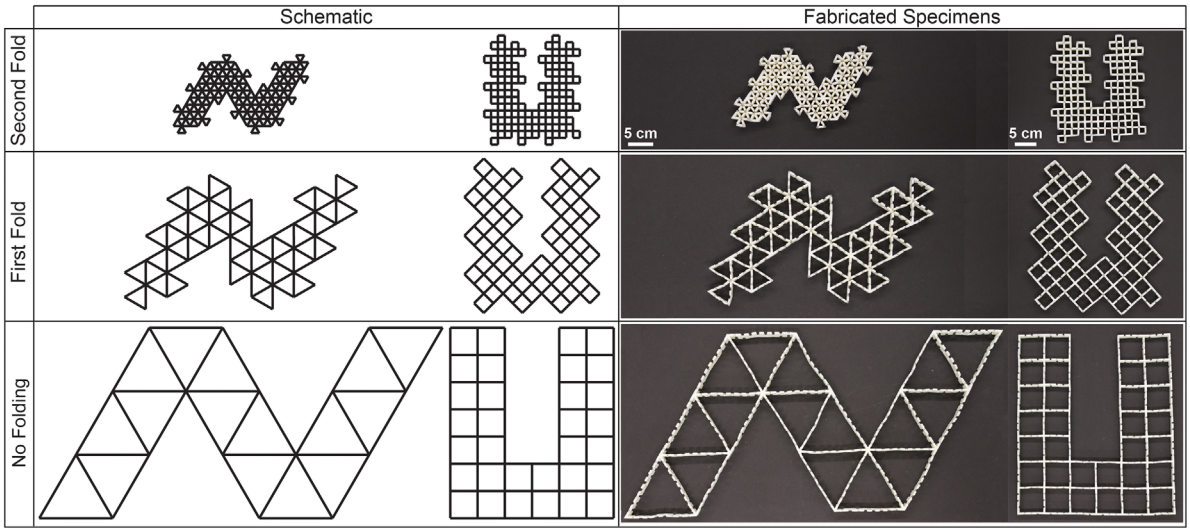

Fig. 2. Schematic and counterpart fabricated specimens showing two lattices with square and triangle grids at different stages of unfolding demonstrating the reversibility of the folding process. Complete unfolding of the triangular grid results in alphabet N, while unfolding of the square grid results in alphabet U (The design is inspired by the abbreviation of Northeastern University–NU).

with triangular grids. In calculating the quasi-static elastic and phononic properties of these lattices, we assumed that the structures are periodic and infinitely extended in two-dimensional space (i.e., we employed periodic boundary conditions). Therefore, the sequence of rotation directions does not affect the "representative volume element" (i.e., RVE or unit cell) (see Supporting Information) of the structures and so the claculated properties.

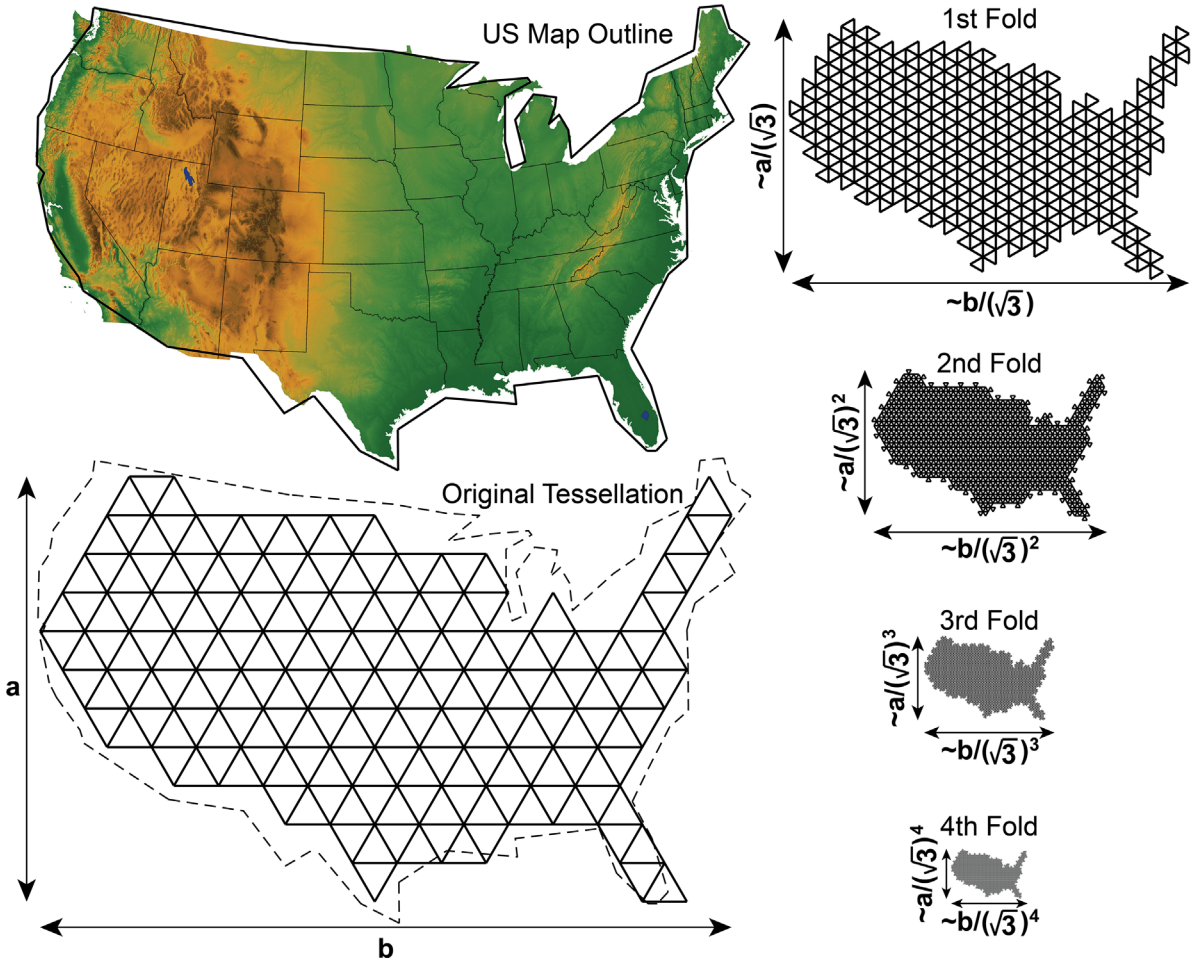

Fig. 3. Folding a tessellated lattice representing the United States map. Triangular grid was used and four levels of folding were performed.

First, we present a closed-form analytical model to link the topology of lattice structure at different folding transition stages to its elastic constants (i.e., Young's modulus, Poisson's ratio, and shear modulus). Frame boundary conditions were imposed on the joints to keep the structure fixed at desired level of folding. We used the energy method (i.e., Castigliano's second theorem[21]) for a representative square grid lattice under in-plane loads, yielding the following closed-form expression of elastic properties of the square grid lattice during i-th level of folding:

$$\frac{E_x}{E_s} = \frac{1}{\left((\cos(\theta_i/2))^2/(t/L_i) + (\sin(\theta_i/2))^2/\left((8/5)(t/L_i)^3\right)\right)} \quad (1)$$

$$\nu_{xy} = -\frac{\left((\sin(\theta_i/2))^2/\left((8/3)(t/L_i)^3\right)\right)}{\left((\cos(\theta_i/2))^2/(t/L_i) + (\sin(\theta_i/2))^2/\left((8/5)(t/L_i)^3\right)\right)} \quad (2)$$

$$\frac{G_{xy}}{E_s} = \frac{0.5}{\left((\cos(\theta_i/2))^2/(t/L_i)^3 + (\sin(\theta_i/2))^2/(t/L_i)\right)} \quad (3)$$

where E_x, ν_{xy}, and G_{xy} are, respectively, the Young's modulus, Poisson's ratio, and shear modulus of the structure measured within the x-y coordinate system aligned with the axes of symmetry of the original structure (i.e., principal directions) throughout folding transition. E_s is the Young's modulus of the parent material, θ_i is the rotation of the pin-joints, and t/L_i is the thickness-to-length ratio of the cell walls at the beginning of the folding ($\theta_i = 0$). Finally, the Young's modulus, along the directions parallel to lattice members was calculated from the transformed compliance tensor of the structure (see Supporting Information for more details). Note that plugging $\theta_i = 0$ into Equations 1–3 will result in t/L_i, 0, and $0.5(t/L_i)^3$, which are the normalized Young's modulus, Poisson's ratio, and shear modulus of a square grid with thickness-to-length ratio of t/L_i subjected to a uniaxial load along the cell walls.[22] The results are graphically plotted in Figure 4a, where the solid lines show the analytical calculations while the markers represent FE results (see Supporting Information for details). The response of the structure at the beginning of the folding transition is characterized by a sharp decrease in Young's modulus due to a transition from a fully stretching-dominated structure (i.e., structures, in which stretching is the dominant deformation mechanism of cell walls) at $\theta_i = 0^\circ$ (i.e., a square grid with an applied load along the cell walls) to a bending-dominated structure (i.e., structures in which bending is the dominant deformation mechanism of cell walls) at $\theta_i \to 90^\circ$. As the folding proceeds to higher levels, the difference between the Young's modulus at $\theta_i = 0^\circ$ and $\theta_i \to 90^\circ$ decreases dramatically (e.g., more than two orders of magnitude for the first level of folding compared to one order of magnitude for the third level). This behavior stems from higher thickness-to-length ratio of the lattice at higher levels of folding, lowering the difference of effective stiffness in the stretching- and bending-dominated structures at $\theta_i = 0^\circ$ and $\theta_i \to 90^\circ$. Moreover, since the Young's modulus of stretching- and bending-dominated structures is, respectively, proportional to their thickness-to-length ratio and its cube,[23] higher folding levels (i.e., greater thickness-to-length ratio, where the thickness is constant, but the length is shorter) will lead to a shift in the entire profile of the Young's modulus to higher values.

In addition to bearing loads, lattice materials can also exhibit rich band structure property during the propagation of small-amplitude elastic waves.[24] Thus, the proposed folding scheme can also be used to tune the band structure[25] for multifunctional applications. Here, we investigate the evolution of bandgaps during the folding transition of square gird lattices. To this end, we assume the structure to be infinitely extended in a two-dimensional space. We investigate the propagation of small-amplitude elastic waves in the lattice structures using FE method and Bloch wave analysis[26] (see Supporting Information for details). In our numerical simulations, we neglect the effects induced by the degrees of freedom of the joints through imposing frame boundary condition on the joints to keep the structure fixed at desired stage of folding – same assumption used in calculating the elastic properties. The lattice members were modeled as Timoshenko beam elements[27] with rectangular cross sections of unit depth. The constituent material was assumed to be aluminum with Young's modulus, $E_s = 71\,\text{GPa}$, Poisson's ratio, $\nu_s = 0.33$, and density, $\rho_s = 2\,700\,\text{kg m}^{-3}$. The relative density (i.e., area fraction: density of the structure divided by the density of the parrent material) of the original square grid was 8%. The frequency of the propagating wave, ω was normalized with respect to the first flexural frequency of a simply supported beam, with length and thickness of those of the original square grid, that is, $\Omega = \omega/\omega_0$, where $\omega_0 = \pi^2\sqrt{E_s t^2/\left(12\rho_s {l_1}^4\right)}$, where t and l_1 are thickness of the structure and length of the original square grid, respectively.

We quantify the topological change of the structure, using the rotation of pin-joints at different levels of folding, θ_1, θ_2, and θ_3. In Figure 4b, we present the evolution of bandgaps for a square based lattice as the values of θ_1, θ_2, and θ_3 increase, respectively, for first, second, and third levels of folding for the range of frequencies $0 \leq \Omega \leq 34.46$. As expected, significant variation of the band structure is evident between folding levels and during the transition. The first folding level shows the presence of distinct band gaps across a large spectrum of frequencies at various stages of the evolution of geometry. This behavior changes completely, as the level of folding advances to the third level. In this level, band gaps disappear completely at lower angles of lattice members and widen and shift to higher frequencies.

The current study proposes a simple and reversible yet effective way to change geometry of the lattice materials dramatically in a controllable fashion. We showed that the proposed folding scheme can be reversibly and numerously

ADVANCED ENGINEERING MATERIALS

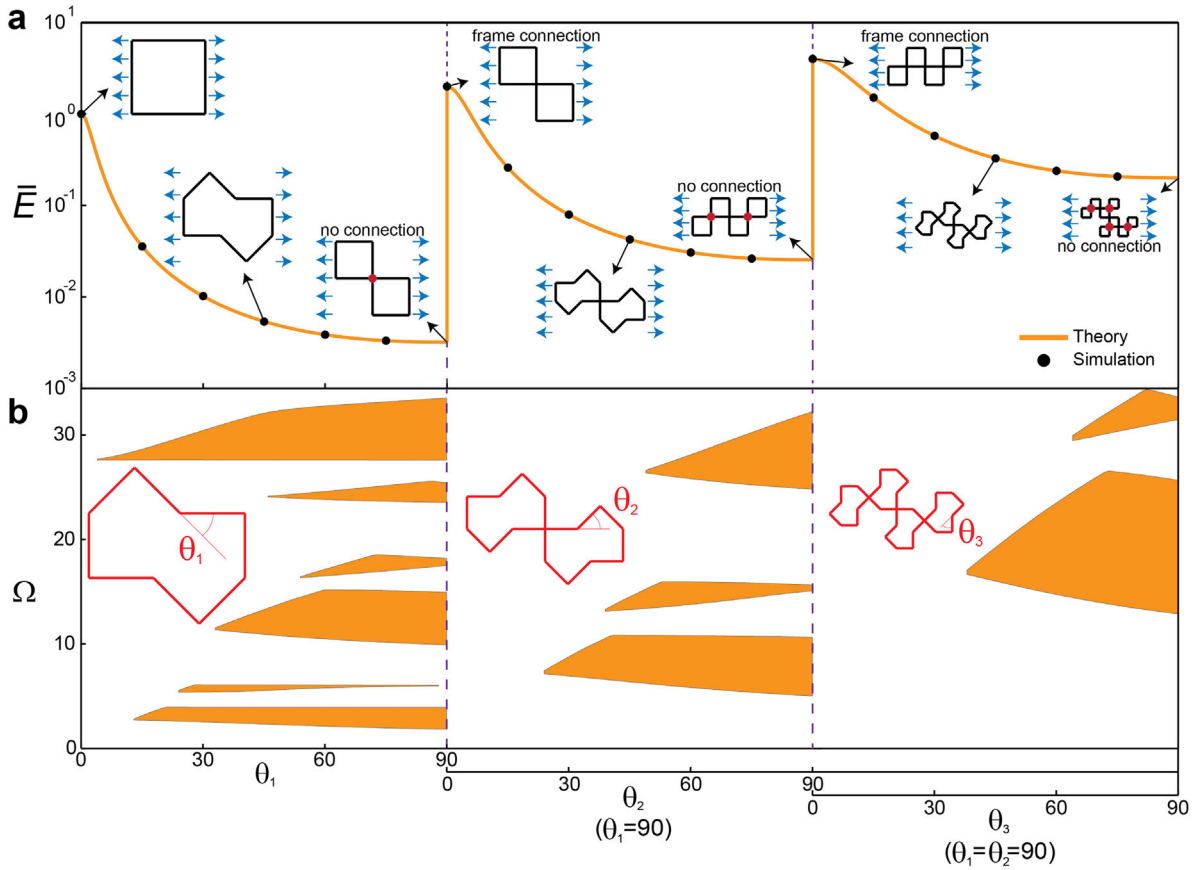

Fig. 4. (a) Young's modulus (normalized with respect to the Young's modulus of the original square grid) and (b) band structure frequency (normalized with respect to the first flexural frequency of a simply supported beam with edge length and thickness of the original square grid) plotted against θ_1, θ_2, and θ_3 (change of angle between lattice members). The relative density of the original square grid is 8%. The red dots on lattice configurations just before $\theta_1 = 90°$, $\theta_2 = 90°$, and $\theta_3 = 90°$ denote the unconnected frame parts.

repeated, until a desired shape of the lattice material is reached. This size-changing concept provides an alternate technique for controlling the underlying topology rapidly and reversibly through simple collapse or expansion of the base lattice. Such dramatic change of size points to potential applications for deployable structures, which can simultaneously benefit from the inherent lightweight and multifunctional characteristics associated with lattice architectures.

However, the main limitation of our proposed lattices is that the hinges must be locked in place for the material to perform structurally as presented, here, for tunable elastic and phononic applications. One possible locking mechanism is to use servo motors in the joints to fold or fix them as needed. Another solution could be using electromagnets in joints and turn them on/off selectively to perform the folding process. However, using these method will add a limitation to the mechanical performance of these lattices due to limitations on electromagnetic holding forces and servo motors maximum torque.

Article first published online: January 09, 2017
Manuscript Revised: December 15, 2016
Manuscript Received: September 12, 2016

[1] D. Mousanezhad, S. Babaee, H. Ebrahimi, R. Ghosh, A. S. Hamouda, K. Bertoldi, A. Vaziri, *Sci. Rep.* **2015**, *5*, 18306.

[2] a) B. Haghpanah, H. Ebrahimi, D. Mousanezhad, J. Hopkins, A. Vaziri, *Adv. Eng. Mater.* **2016**, *18*, 643; b) Y. Cho, J. H. Shin, A. Costa, T. A. Kim, V. Kunin, J. Li, S. Y. Lee, S. Yang, H. N. Han, I. S. Choi, D. J. Srolovitz, *PNAS* **2014**, *111*, 49.

[3] a) E. Brown, N. Rodenberg, J. Amend, A. Mozeika, E. Steltz, M. R. Zakin, H. Lipson, H. M. Jaeger, *PNAS* **2010**, *107*, 18809; b) J. R. Amend, E. Brown, N. Rodenberg, H. M. Jaeger, H. Lipson, *IEEE Tran. Rob.* **2012**, *28*, 341; c) N. G. Cheng, M. B. Lobovsky, S. J. Keating, A. M. Setapen, K. I. Gero, A. E. Hosoi, K. D. Iagnemma, *IEEE Int. Conf. Rob. Autom. (Icra)* **2012**, 4328. doi: 10.1109/ICRA.2012.6225373; d) K. Gilpin, A. Knaian, D. Rus, *IEEE Int. Conf. Rob. Autom.* **2010**, 2485. doi: 10.1109/ROBOT.2010.5509817; e) B. Piranda, G. J. Laurent, J. Bourgeois, C. Clevy, S. Mobes, N. Le Fort-Piat, *Mechatronics* **2013**, *23*, 906; f) H. X. Wei, Y. D. Chen, J. D. Tan, T. M. Wang, *IEEE-ASME Tran. Mech.* **2011**, *16*, 745.

[4] J. L. Silverberg, A. A. Evans, L. McLeod, R. C. Hayward, T. Hull, C. D. Santangelo, I. Cohen, *Science* **2014**, *345*, 647.
[5] S. Felton, M. Tolley, E. Demaine, D. Rus, R. Wood, *Science* **2014**, *345*, 644.
[6] E. Hawkes, B. An, N. M. Benbernou, H. Tanaka, S. Kim, E. D. Demaine, D. Rus, R. J. Wood, *PNAS* **2010**, *107*, 12441.
[7] a) S. Jacobs, C. Coconnier, D. di Maio, F. Scarpa, M. Toso, J. Martinez, *Smart Mater. Struct*. **2012**, *21*, 075013; b) J. Rossiter, K. Takashima, F. Scarpa, P. Walters, T. Mukai, *Smart Mater. Struct*. **2014**, *23*, 045007; c) Y. Chen, Z. You, T. Tarnai, *Int. J. Solids Struct*. **2005**, *42*, 2287.
[8] L. Puig, A. Barton, N. Rando, *Acta Astronaut*. **2010**, *67*, 12.
[9] a) Q. Ge, H. J. Qi, M. L. Dunn, *Appl. Phys. Lett*. **2013**, *103*, 131901. doi: 10.1063/1.4819837; b) S. Tibbits, *Archit. Design* **2014**, *84*, 116.
[10] a) C. H. Ahn, C. Jin-Woo, G. Beaucage, J. H. Nevin, L. Jeong-Bong, A. Puntambekar, J. Y. Lee, *Proc. IEEE* **2004**, *92*, 154; b) C. H. Ahn, A. Puntambekar, S. M. Lee, H. J. Cho, C. C. Hong, in *Micro Total Analysis Systems 2000* (Eds: A. Berg, W. Olthuis, P. Bergveld), Springer, Dordrecht, Netherlands **2000**, p. 205.
[11] a) A. Metcalfe, A. C. Desfaits, I. Salazkin, L. Yahia, W. M. Sokolowski, J. Raymond, *Biomaterials* **2003**, *24*, 1681; b) K. Kuribayashi, K. Tsuchiya, Z. You, D. Tomus, M. Umemoto, T. Ito, M. Sasaki, *Mater. Sci. Eng. A* **2006**, *419*, 131; c) L. de Nardo, S. Bertoldi, M. C. Tanzi, H. J. Haugen, S. Fare, *Smart Mater. Struct*. **2011**, *20*, 035004.
[12] Z. You, S. Pellegrino, *AIAA J*. **1996**, *34*, 813.
[13] Z. You, S. Pellegrino, *AIAA J*. **1997**, *35*, 8.
[14] A. G. Tibert, S. Pellegrino, *J. Spacecr. Rockets* **2002**, *39*, 701.
[15] a) D. J. Rohweller, *Proc. 36th Aerospace Mechanisms Symposium, Glenn Research Center*, NASA Center for Aerospace Information, Hanover, MD, **2002**, 155; b) M. Schenk, A. D. Viquerat, K. A. Seffen, S. D. Guest, *J. Spacecr. Rockets* **2014**, *51*, 762.
[16] J. K. H. Lin, C. F. Knoll, C. E. Willey, *Proc. 47th AIAA/ASME/ASCE/AHS/ASC Structures, Structural Dynamics, and Materials Conf*. American Institute of Aeronautics and Astronautics, Reston, VA, **2006**.
[17] G. Tibert, *PhD dissertation*, Department of Mechanics, Royal Institute of Technology, Stockholm, Sweden **2002**.
[18] a) J. S. Zhao, F. Chu, Z. J. Feng, *Mech. Machine Theory* **2009**, *44*, 324; b) T. Langbecker, *Int. J. Space Struct*. **1999**, *14*, 1.
[19] a) L. H. Dudte, E. Vouga, T. Tachi, L. Mahadevan, *Nat. Mater*. **2016**, *15*, 583; b) J. T. Overvelde, T. A. de Jong, Y. Shevchenko, S. A. Becerra, G. M. Whitesides, J. C. Weaver, C. Hoberman, K. Bertoldi, *Nat. Commun*. **2016**, *7*, 10929. doi: 10.1038/ncomms10929; c) M. Schenk, S. D. Guest, *PNAS* **2013**, *110*, 3276; d) C. D. Onal, R. J. Wood, D. Rus, *IEEE/ASME Tran. Mech*. **2013**, *18*, 430.
[20] a) T. T. Michael, M. F. Samuel, M. Shuhei, A. Daniel, R. Daniela, J. W. Robert, *Smart Mater. Struct*. **2014**, *23*, 094006; b) J. H. Na, A. A. Evans, J. Bae, M. C. Chiappelli, C. D. Santangelo, R. J. Lang, T. C. Hull, R. C. Hayward, *Adv. Mater*. **2015**, *27*, 79.
[21] A. P. Boresi, R. J. Schmidt, O. M. Sidebottom, *Advanced Mechanics of Materials, Vol. 6*, Wiley New York, New York, NY **1993**.
[22] D. Mousanezhad, B. Haghpanah, R. Ghosh, A. S. Hamouda, H. Nayeb-Hashemi, A. Vaziri, *Theor. Appl. Mech. Lett*. **2016**, *6*, 2.
[23] L. J. Gibson, M. F. Ashby, *Cellular Solids: Structure and Properties*, Cambridge university press, Cambridge, United Kingdom **1997**.
[24] D. Mousanezhad, S. Babaee, R. Ghosh, E. Mahdi, K. Bertoldi, A. Vaziri, *Phys. Rev. B* **2015**, *92*, 5.
[25] M. Schaeffer, M. Ruzzene, *J. Appl. Phys*. **2015**, *117*, 19.
[26] L. Brillouin, *Wave Propagation in Periodic Structures: Electric Filters and Crystal Lattices*, Courier Corporation, Dover Publications, Inc., Mineola, NY **2003**.
[27] D. Logan, *A First Course in the Finite Element Method*, Cengage Learning, Stamford, CT **2011**.

